Supporting Information

Three-Dimensional Iron-Cobalt Phosphides Nanosheets on Nickel Oxide Nanoparticles for Improved Glucose Oxidation Reaction

*Sundaramoorthy Marimuthu†, Harichandana Anoopkumar† and Govindhan Maduraiveeran**

Materials Electrochemistry Laboratory, Department of Chemistry, SRM Institute of Science and Technology, Kattankulathur - 603 203, Chengalpattu, Tamil Nadu, India.

**Corresponding Author: E-mail: maduraig@srmist.edu.in & pgmadura@yahoo.co.in; Tel. Phone: +044 2741 62628*

†: Equal Author Contributions

Table S1. Comparison of the GOR performance of the 3D FeCoP NS|NiO NP heterostructures with the recently reported catalysts.

S.No	Materials	E_{pa} (V)	Ref. electrode	Electrolyte	Ref.
1	$NiCo_2O_4$	1.42	RHE	1.0 M KOH	S1
2	$CuS@Ni(OH)_2/CC$	0.49	Ag/AgCl	0.1 M NaOH	S2
3	PdSn/C	0.11	Hg/HgO	0.5 M KOH	S3
4	Pt/Ni nanowires	1.52	RHE	0.1 M NaOH	S4
5	Pd_3Sn/Se-C	0.110	Ag/AgCl	0.1 M KOH	S5
6	FeS NS|NF	0.34	Ag/AgCl	1.0 M KOH	S6
7	Pd/C	0.25	Hg/HgO	0.1 M NaOH	S7
8	**3D FeCoP NS|NiO NP**	**0.22**	**Ag/AgCl**	**1.0 M KOH**	**This work**

Table S2. EIS data derived from Nyquist plots 3D FeCoP NS|NiO NP, 3D FeP NS|NiO NP, and 3D CoP NS|NiO NP electrodes.

Electrodes	E_{app} **/ V**	R_s **[Ω]**	R_p **[kΩ]**	C **[μF]**
3D FeCoP NS|NiO NP	0.20	9.78	5.35	3.74
	0.24	13.50	10.99	7.25
	0.27	56.77	7.64	11.70
	0.29	36.11	5.91	9.54
3D FeP NS|NiO NP	0.20	47.95	11.16	3.19
	0.24	35.26	8.64	4.62
	0.27	14.16	9.88	7.19
	0.29	7.05	14.21	17.74
3D CoP NS|NiO NP	0.20	39.78	11.18	2.00
	0.24	44.72	7.33	4.32
	0.27	8.94	4.36	5.78
	0.29	12.28	48.51	8.24

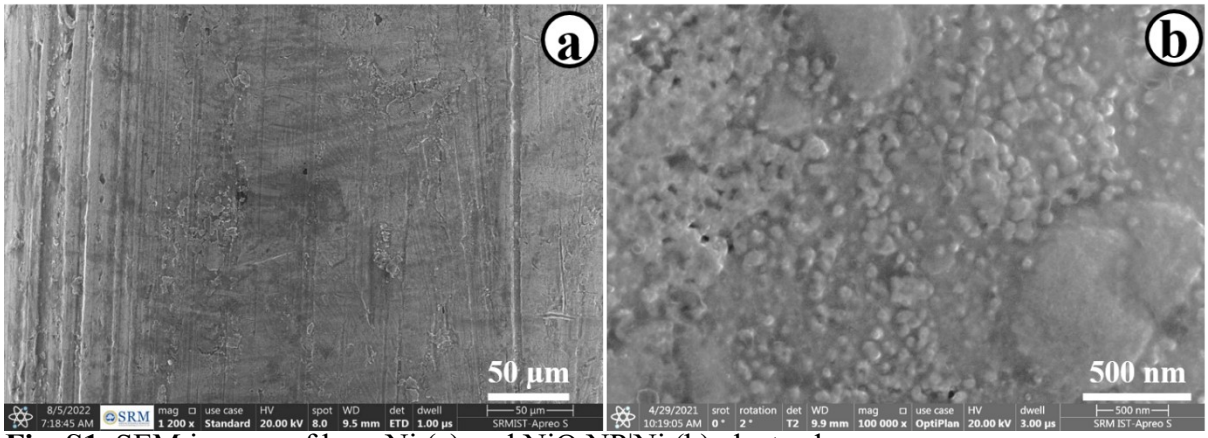

Fig. S1. SEM images of bare Ni (a) and NiO NP|Ni (b) electrodes.

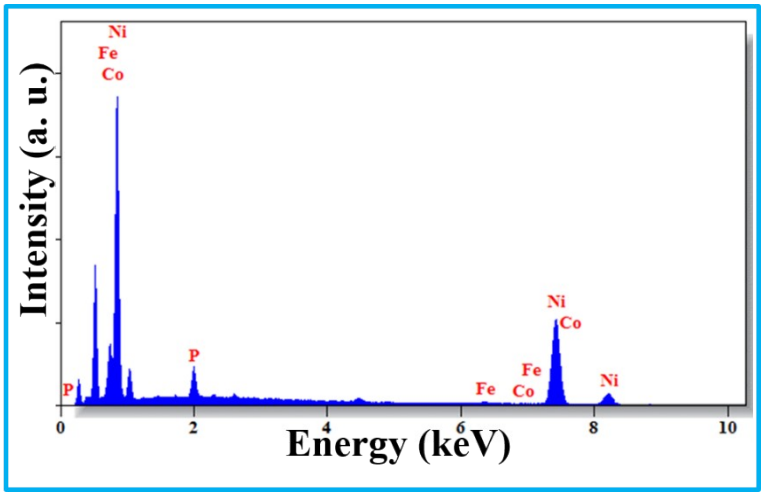

Fig. S2. SEM-EDX analysis of 3D FeCoP NS|NiO NP heterostructures.

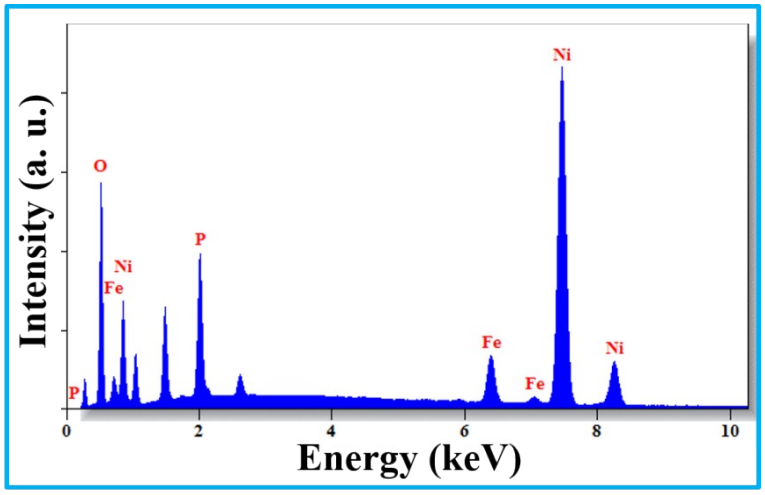

Fig. S3. EDX analysis of 3D FeP NS|NiO NP heterostructures.

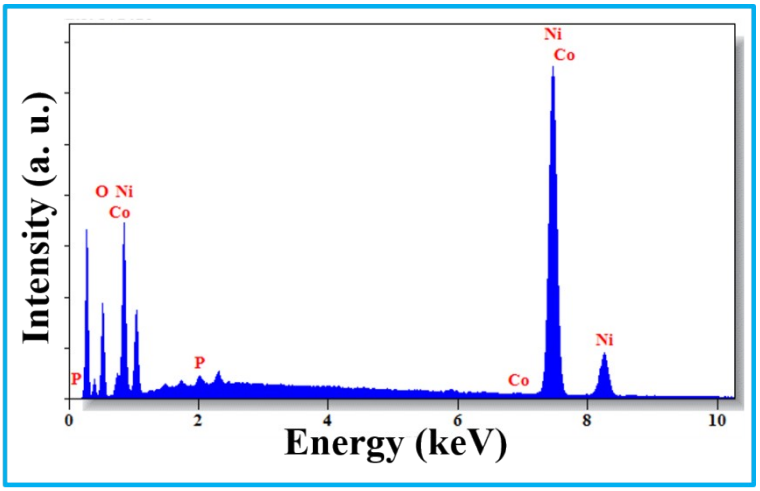

Fig. S4. EDX analysis of CoP NS|NiO NP heterostructures.

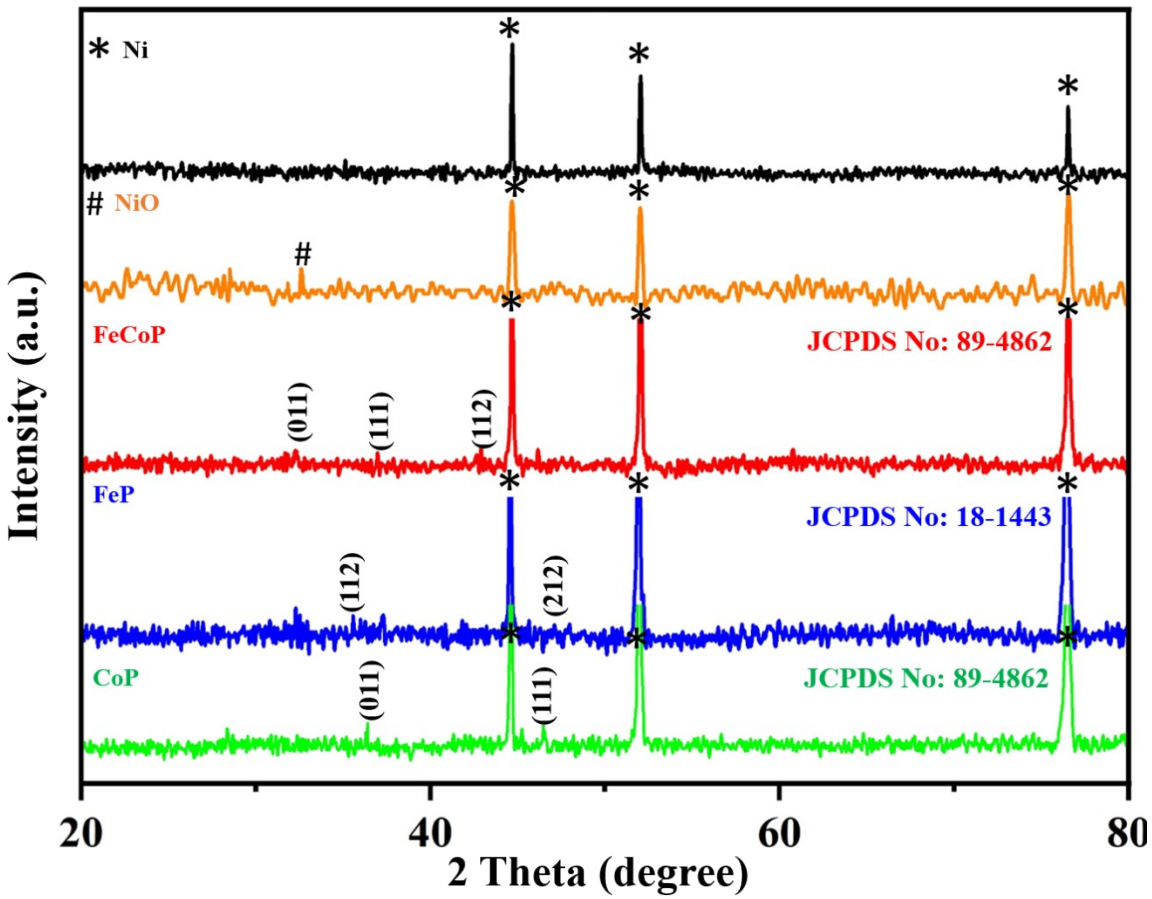

Fig. S5. XRD patterns of the developed electrodes, such as bare Ni (black curve), NiO|Ni (orange curve), 3D FeCoP NS|NiO NP (red curve), 3D FeP NS|NiO NP (blue curve), 3D CoP NS|NiO NP (green curve).

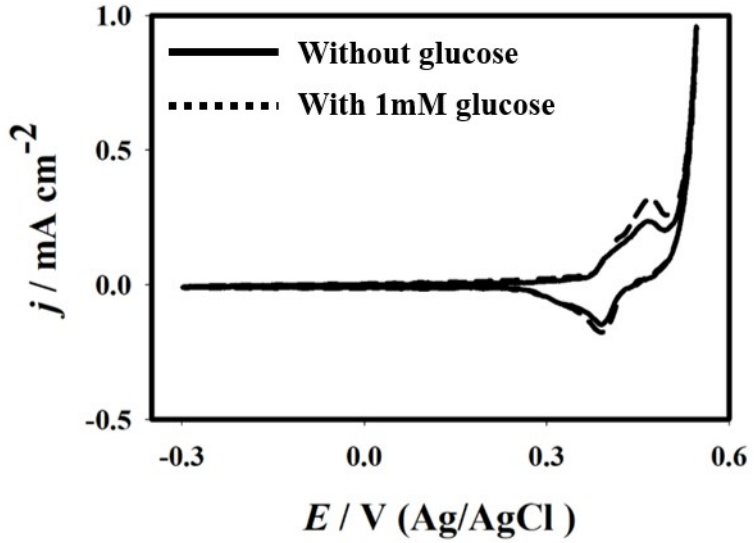

Fig. S6. CV curves of bare Ni electrode recorded without addition (black) and with the addition (doted) of 1.0 mM glucose in 1.0 m KOH at a scan rate of 10.0 mV s^{-1}.

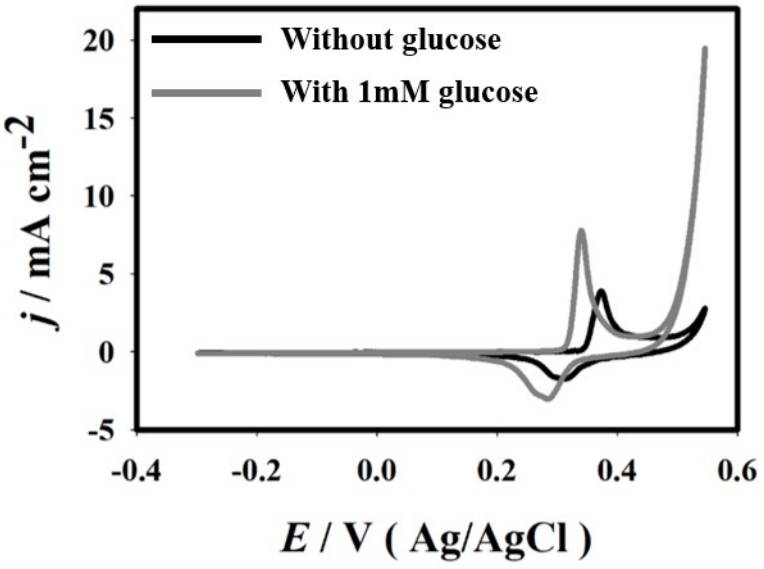

Fig. S7. CV curves of NiO NP|Ni electrode recorded without addition (black) and with the addition (grey) of 1.0 mM glucose in 1.0 m KOH at a scan rate of 10.0 mV s^{-1}.

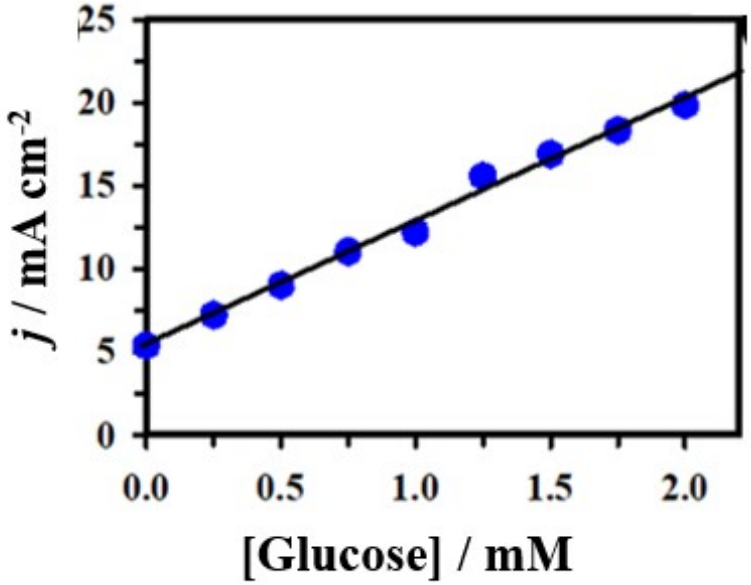

Fig. S8. The plot of anodic current density *vs*. various concentrations of glucose at the 3D FeP NS|NiO NP electrode.

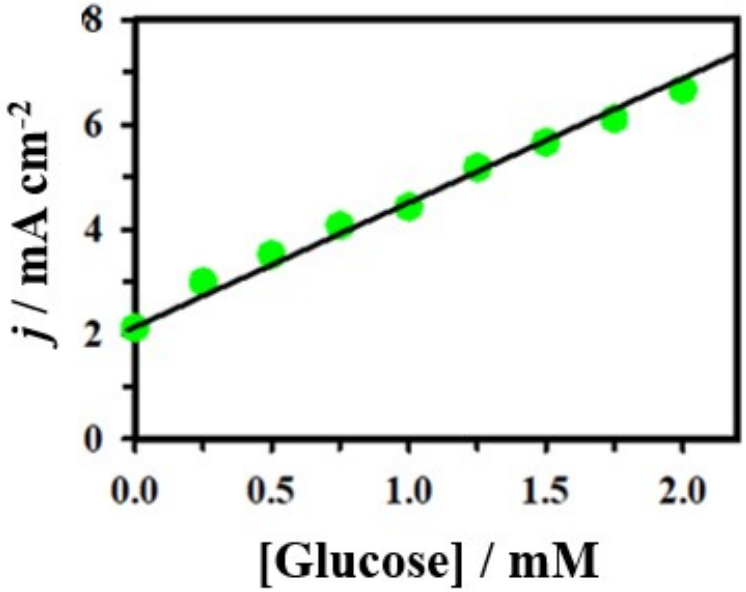

Fig. S9. The plot of anodic current density against various concentrations of glucose at the 3D CoP NS|NiO NP electrode.

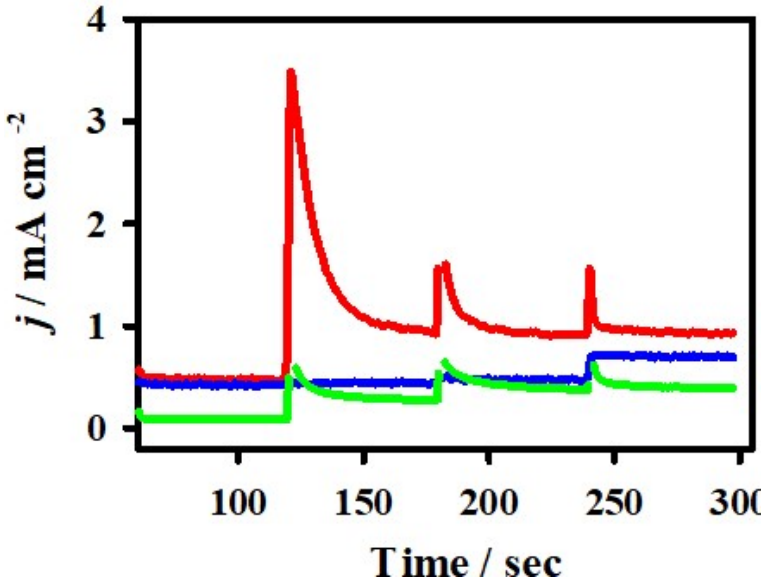

Fig. S10. CA response of the 3D FeCoP NS|NiO NP (red curve), 3D FeP NS|NiO NP (blue curve), and 3D CoP NS|NiO NP electrodes at different applied potentials.

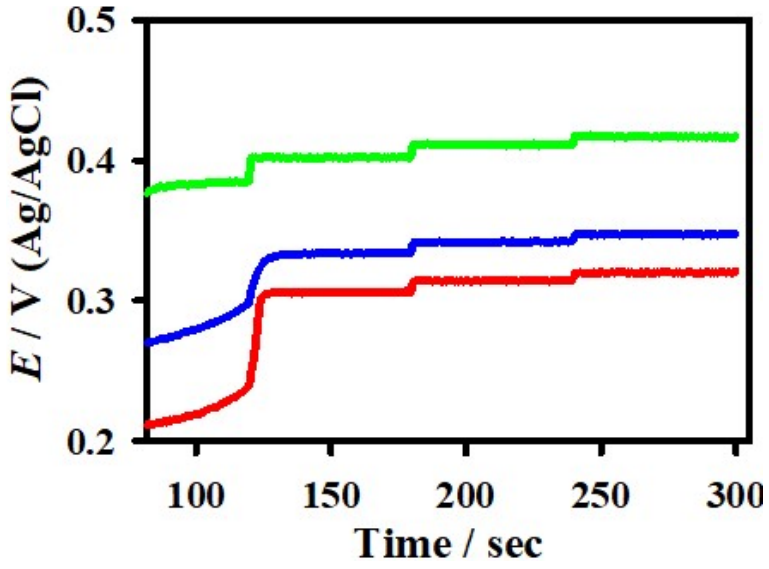

Fig. S11. CP response of the 3D 3FeCoP NS|NiO NP (red curve), 3D FeP NS|NiO NP (blue curve), and 3D CoP NS|NiO NP (green) electrodes at different applied currents.

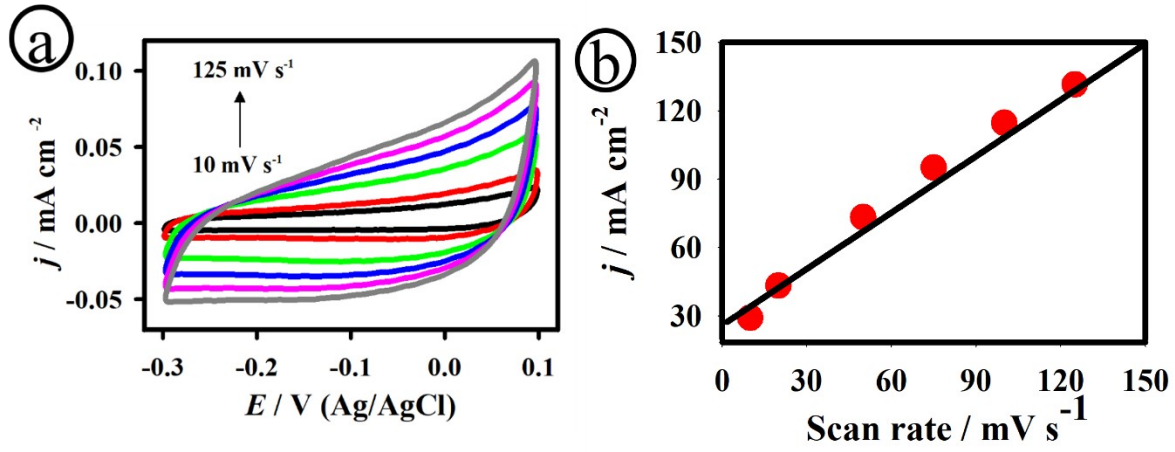

Fig. S12. CV curves of 3D FeCoP NS|NiO NP electrode recorded in 1.0 M KOH solution at different scan rates from 10 to 125 mV s^{-1} (a) and the corresponding plot of anodic current density vs scan rate (b).

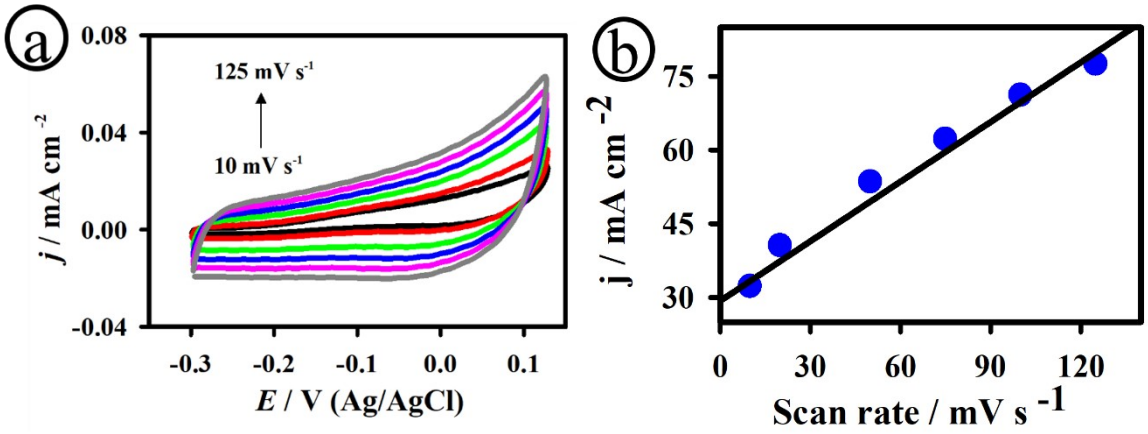

Fig. S13. CV curves of 3D FeP NS|NiO NP electrode recorded in 1.0 M KOH solution at different scan rates from 10 to 125 mV s^{-1} (a) and the corresponding plot of anodic current density vs scan rate (b).

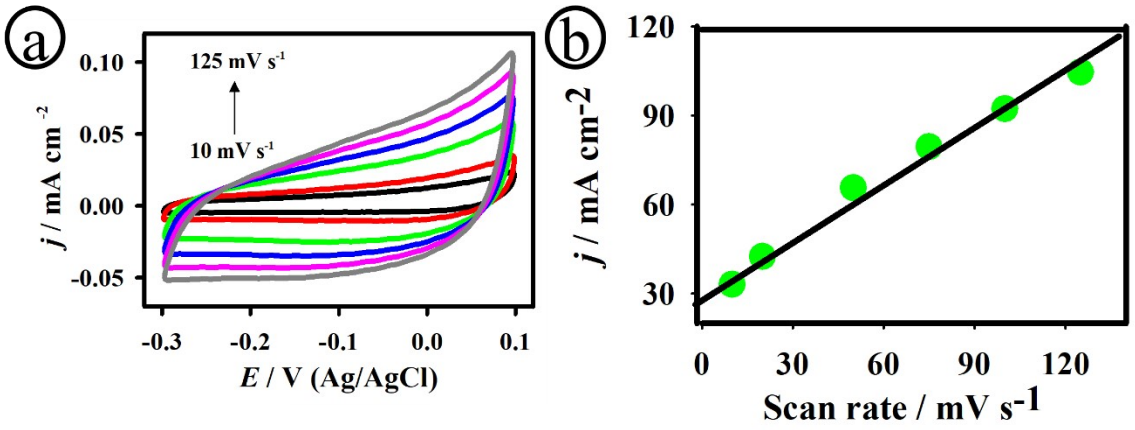

Fig. S14. CV curves of 3D CoP NS|NiO NP electrode recorded in 1.0 M KOH solution at different scan rates from 10 to 125 mV s^{-1} (a), and the corresponding plot of anodic current density vs scan rate (b).

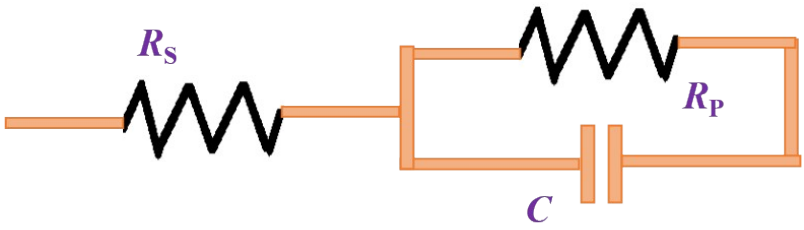

Fig. S15. Fitted electronic equivalent circuit for **Fig. 7.**

Reference

S1 R. Elakkiya and G. Maduraiveeran, *New J. Chem.*, 2019, **43**, 14756–14762.

S2 G. Siva, M. A. Aziz and G. Gnana kumar, *ACS Sustain. Chem. Eng.*, 2018, **6**, 5929–5939.

S3 A. Brouzgou, S. Song and P. Tsiakaras, *Appl. Catal. B Environ.*, 2014, **158**–**159**, 209–216.

S4 S. S. Mahshid, S. Mahshid, A. Dolati, M. Ghorbani, L. Yang, S. Luo and Q. Cai, *Electrochim. Acta*, 2011, **58**, 551–555.

S5 W. Wang, Y. Dong, L. Xu, W. Dong, X. Niu and Z. Lei, *Electrochim. Acta*, 2017, **244**, 16–25.

S6 A. Shankar and G. Maduraiveeran, *Bull. Mater. Sci.*, 2022, **45**, 148.

S7 D. Chai, W. Wang, F. Wang, Y. Kang, Y. Yang and Z. Lei, *Electrochim. Acta*, 2016, **189**, 295–302.